SUPPLEMENTAL FIGURE LEGENDS

Supplemental Figure S1. RBPJ correlates with BTIC marker expression. A-D. The TCGA GBM dataset was downloaded and correlations analyzed by R. RBPJ mRNA levels were highly correlated with (A) Olig2, (B) Sox2, (C) CD133, and (D) Sox4 levels. E. RBPJ is preferentially expressed in proneural glioblastomas. The glioblastoma TCGA dataset was interrogated for RBPJ mRNA expression segregated by transcriptional profile. The proneural tumors were further divided into G-CIMP (glioma CpG-island methylator phenotype) or non-G-CIMP. **, $p < 0.01$. ****, $p < 0.0001$. *****, $p < 0.00001$.

Supplemental Figure S2. Targeting RBPJ induces BTIC apoptosis. A. 3691 BTICs were transduced with shCONT, shRBPJ-1, or shRBPJ-2. Lysates were prepared and immunoblotted with the indicated antibodies. shRNA-mediated knockdown of RBPJ was associated with increased cleaved (activated) PARP. B. 3691 BTICs were transduced with shCONT, shRBPJ-1, or shRBPJ-2. Apoptosis measured by Annexin V staining. Data are presented as mean ± SEM (two-way ANOVA; **, $p < 0.01$; $n = 3$).

Supplemental Figure S3. Targeting RBPJ does not affect non-BTIC proliferation. Non-BTICs (Top, 3691; Bottom, 4121) were transduced with shCONT, shRBPJ-1, or shRBPJ-2. Cell proliferation was measured by CellTiter-Glo.

Supplemental Figure S4. RBPJ induces transcriptional profiles in BTICs distinct from Notch activation. A. In parallel experiments, 3691 BTICs were either treated with DAPT (at either 5 μM or 10 μM) vs. vehicle control (DMSO) or transduced with shRBPJ vs. shCONT. RNA-Seq was performed and the results displayed as a heat map with normalization to the relevant control. Selected genes are displayed based on biologic processes. B. 3691 BTICs were transduced with shCONT, shRBPJ-1, or shRBPJ-2. Gene expression was analyzed by real-time qPCR (two-way ANOVA; **, $p < 0.01$; n = 3). C. 3691 BTICs were treated with vehicle control (DMSO) or DAPT (5 or 10 μM). Gene expression was analyzed by real-time qPCR (two-way ANOVA; **, $p < 0.01$; n = 3).

Supplemental Figure S5. Transcriptomic profiles in BTICs subjected to RBPJ knockdown, DAPT treatment alone, or combined conditions. A. Ranked list of genes based on their correlation with PC3 for 4121 BTICs based on RNA sequencing after transduction with either shCONT or shRBPJ and treatment with either vehicle control (DMSO) or DAPT treatment. All genes with $p < 0.05$ were first identified and further narrowed to genes with positive or negative correlations with $p < 0.01$. B. Genetic programs associated with genes correlated with RBPJ knocked-down in 4121 BTICs. C. Genetic programs associated with genes correlated with RBPJ knocked-down 4121 BTICs treated with DAPT (5 μM).

Supplemental Figure S6. RBPJ binds to the FOXM1 and OLIG2 promoters independently from Notch activation. A. Cross-linked chromatin was prepared from 3691 BTICs or Non-BTICs then

immunoprecipitated with an anti-RBPJ antibody followed by real-time PCR using primers specific to the indicated regions of FOXM1 promoter (Student's t-test; n = 3). B. RNA expression (by FPKM) in 3691 BTICs of stemness genes bound (red) or not bound (blue) to RBPJ. Median, 75 % and 25 % quartiles demarcated for each group. Median for bound genes was FPKM of 64, while it was 5 for non-bound genes. Mean for bound genes was FPKM of 50, while it was 10 for non-bound genes. C. Cross-linked chromatin from 3691 or 4121 BTICs was prepared then immunoprecipitated with an anti-RBPJ antibody followed by real-time PCR using primers specific to the indicated regions of OLIG2 promoter (Student's t-test; n = 3). D. Cross-linked chromatin was prepared from 3691 BTICs treated with DAPT (5 μM) or vehicle control (DMSO), then immunoprecipitated with an anti-RBPJ antibody, followed by real-time PCR using primers specific to the indicated regions of FOXM1, OLIG2 promoters (n = 3).

Supplemental Figure S7. RBPJ binds to CDK9 and LSD1. A. Lysates of 3691 cells transfected with HA-RBPJ were immunoprecipitated with anti-HA antibody followed by mass spectrum analysis. The spectral identification of peptide HENVVNLIEICR (CDK9: 75-86AA) is shown. B. Lysates of 3691 non-BTICs transfected with HA-RBPJ were immunoprecipitated with anti-HA antibody followed by immunoblotting for LSD1.

Supplemental Figure S8. c-Myc regulates RBPJ expression. The WashU EpiGenome Brower was interrogated at the promoter region of RBPJ for c-Myc genomic binding in human

embryonic stem cells in association with the active transcriptional mark of histone 3 lysine 27 acetylation (H3K27ac). MYC binding co-localized with H3K27ac at the RBPJ locus.

Supplemental Figure S9. Ingenuity Pathway Analysis (IPA) of RBPJ in normal/neural stem cells vs. BTIC. RBPJ-interacting proteins were inquired using IPA tools such as Pathway Explorer (Qiagen). Proteins having been show to directly interact with RBPJ or its promoter were queried. Furthermore, pathway discovery tools were used to identify connectivity between normal stem cell and cancer stem cell pathways. Blue: pathways involved in neural stem cells. Red: pathways involved in brain tumors and BTICs. Dotted line: causal relationship. Solid line: direct interaction between factors or with promoters.

Supplemental Figure S10. Proposed model of RBPJ function in tumor initiating cells.

Figure S1

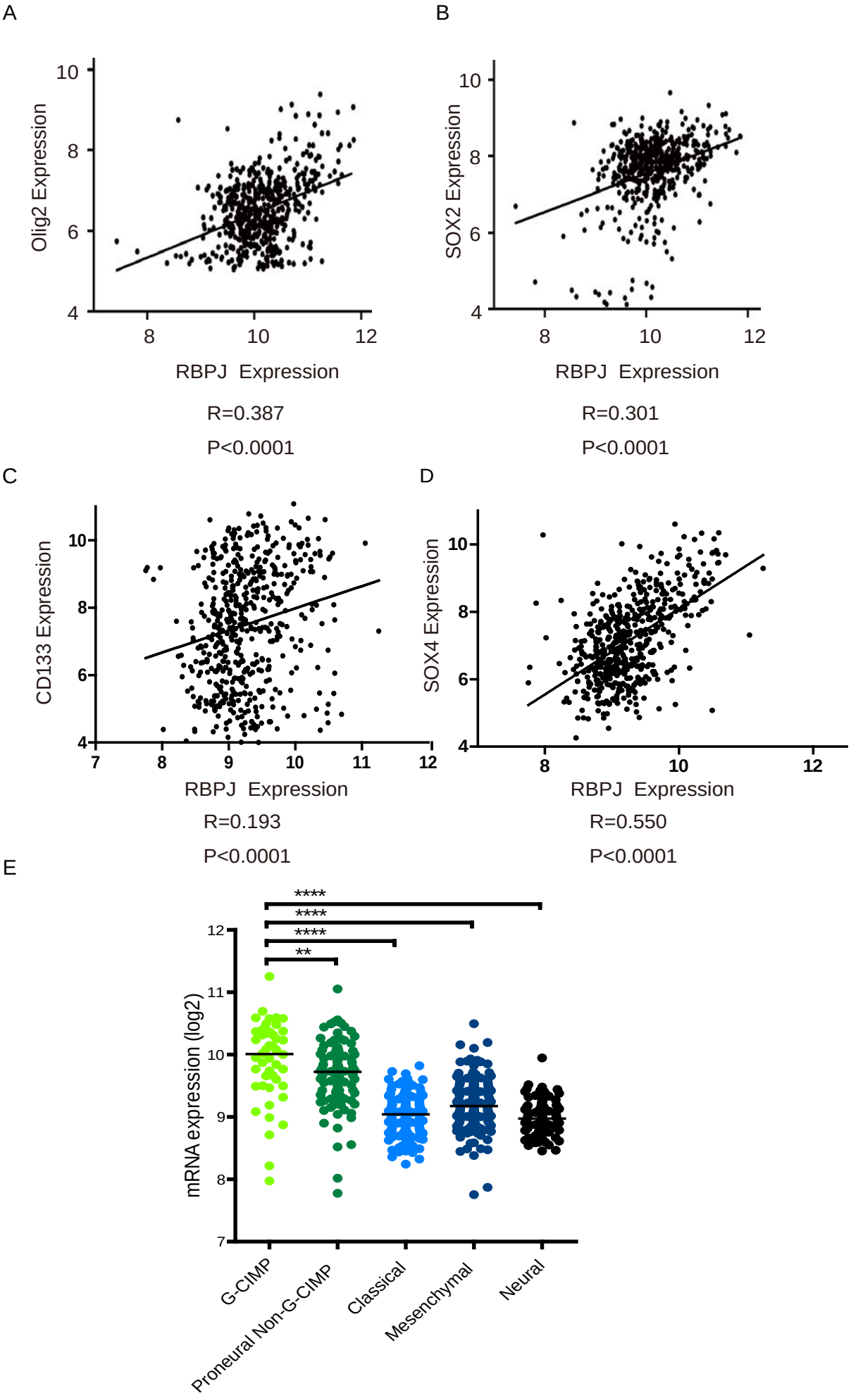
A
Olig2 Expression
RBPJ Expression
R=0.387
P<0.0001
B
SOX2 Expression
RBPJ Expression
R=0.301
P<0.0001
C
CD133 Expression
RBPJ Expression
R=0.193
P<0.0001
D
SOX4 Expression
RBPJ Expression
R=0.550
P<0.0001
E
mRNA expression (log2)
****
****
****
**
G-CIMP
Proneural
Non-G-CIMP
Classical
Mesenchymal
Neural

Figure S2

A

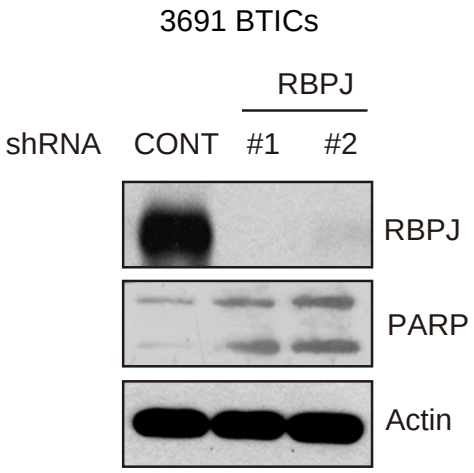
3691 BTICs
RBPJ
shRNA
CONT
#1
#2
RBPJ
PARP
Actin

B

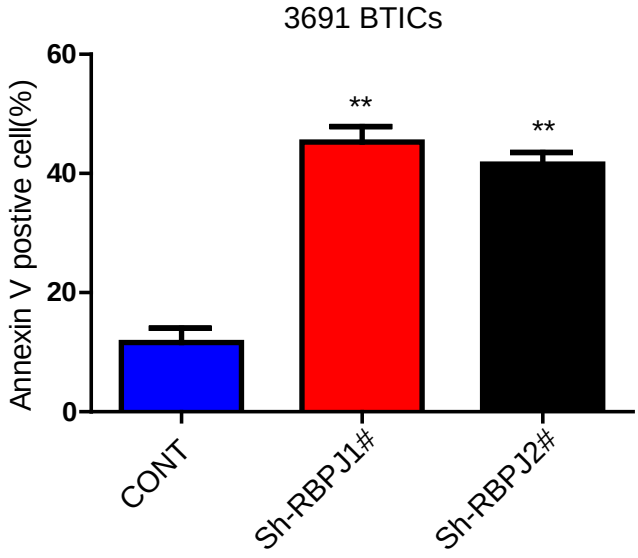
3691 BTICs
Annexin V postive cell(%)
60
40
20
0
**
**
CONT
Sh-RBPJ1#
Sh-RBPJ2#

Figure S3

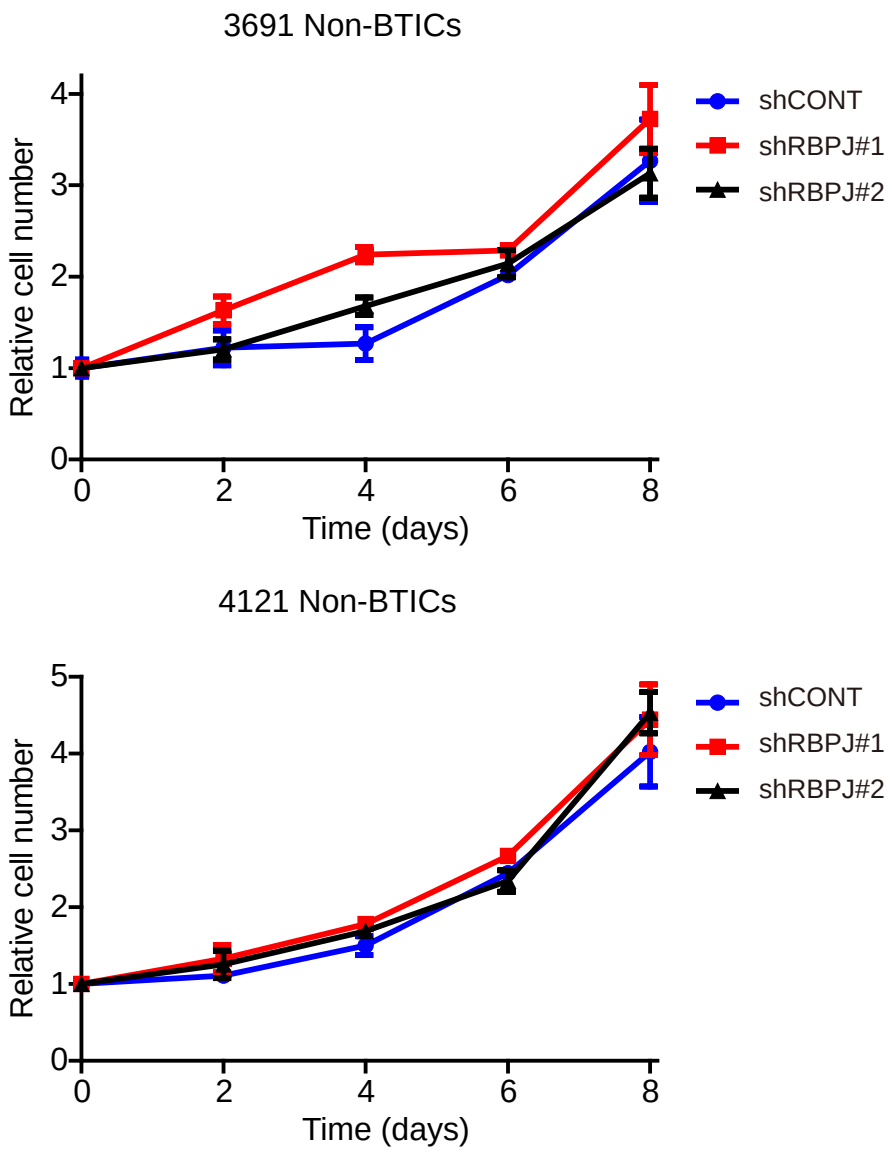
3691 Non-BTICs
Relative cell number
Time (days)
shCONT
shRBPJ#1
shRBPJ#2
4121 Non-BTICs
Relative cell number
Time (days)
shCONT
shRBPJ#1
shRBPJ#2

Figure S4

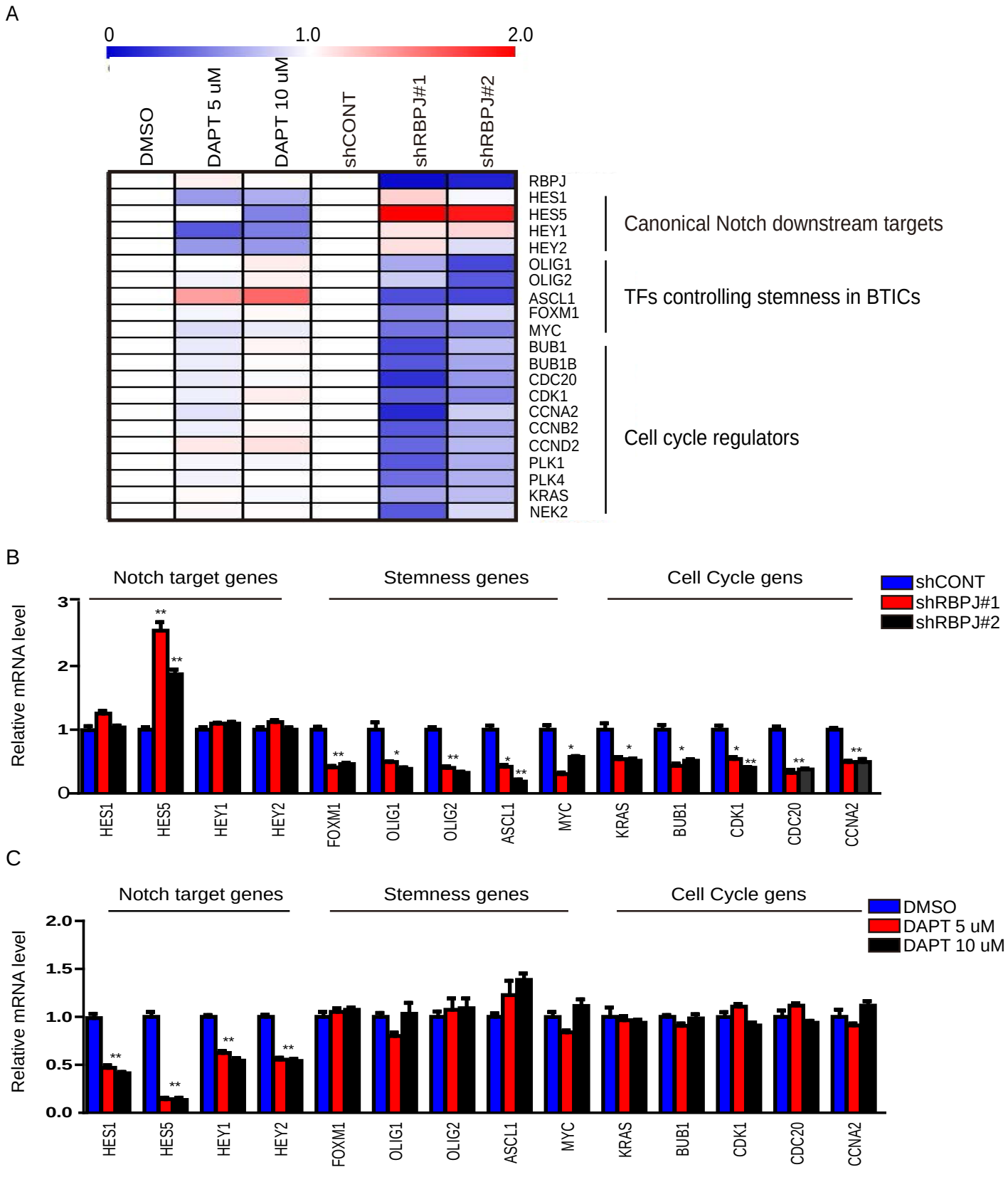
A
0
1.0
2.0
DMSO
DAPT 5 uM
DAPT 10 uM
shCONT
shRBPJ#1
shRBPJ#2
RBPJ
HES1
HES5
HEY1
HEY2
OLIG1
OLIG2
ASCL1
FOXM1
MYC
BUB1
BUB1B
CDC20
CDK1
CCNA2
CCNB2
CCND2
PLK1
PLK4
KRAS
NEK2
Canonical Notch downstream targets
TFs controlling stemness in BTICs
Cell cycle regulators
B
Notch target genes
Stemness genes
Cell Cycle gens
shCONT
shRBPJ#1
shRBPJ#2
Relative mRNA level
HES1
HES5
HEY1
HEY2
FOXM1
OLIG1
OLIG2
ASCL1
MYC
KRAS
BUB1
CDK1
CDC20
CCNA2
C
Notch target genes
Stemness genes
Cell Cycle gens
DMSO
DAPT 5 uM
DAPT 10 uM
Relative mRNA level

Figure S5

A

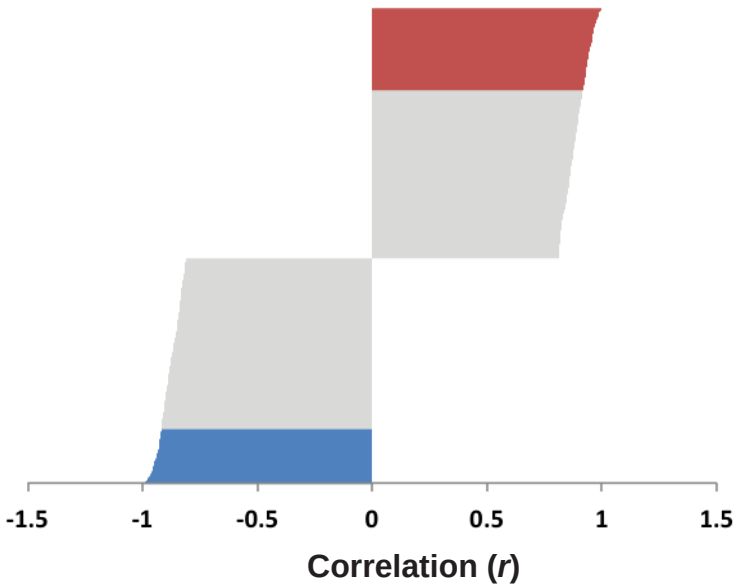

B

C

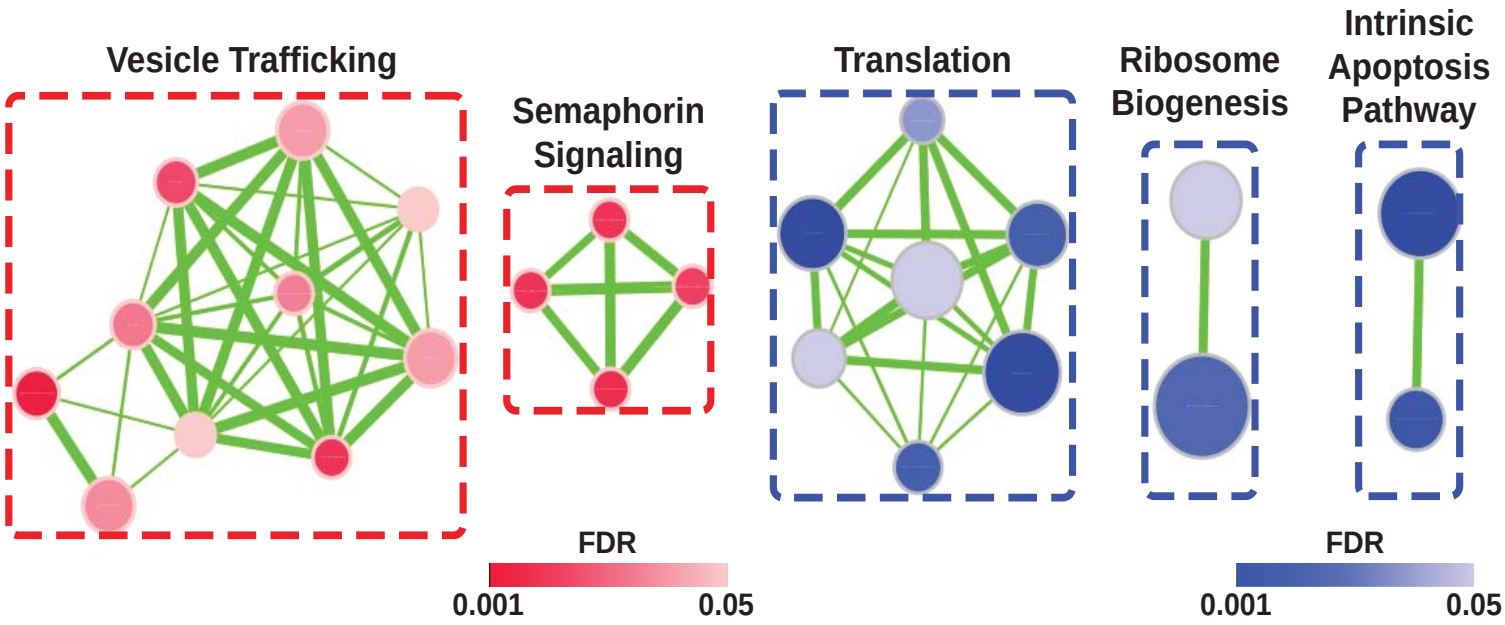

Figure S6

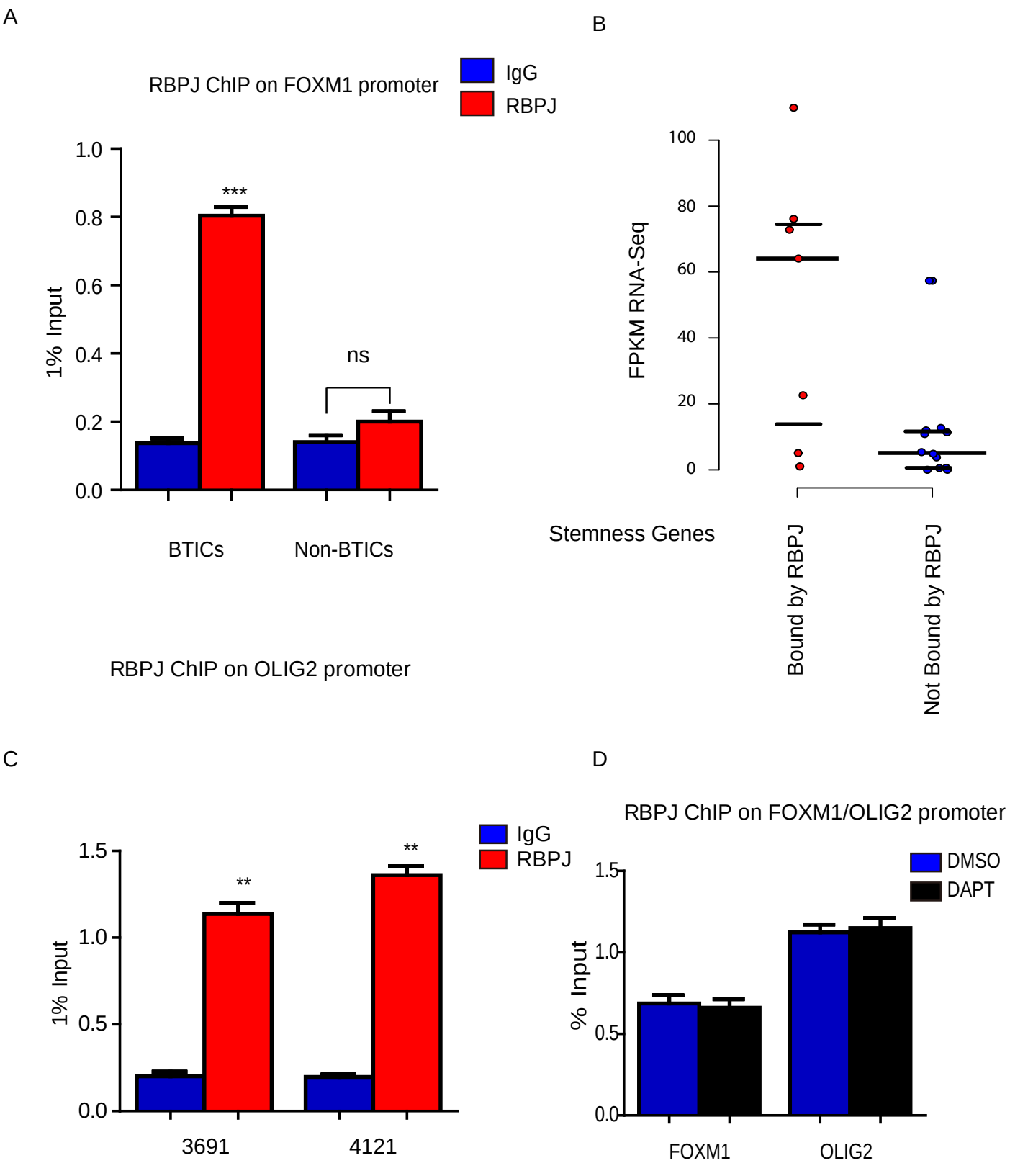
A
RBPJ ChIP on FOXM1 promoter
IgG
RBPJ
1% Input
1.0
0.8
0.6
0.4
0.2
0.0
***
ns
BTICs
Non-BTICs
B
FPKM RNA-Seq
100
80
60
40
20
0
Stemness Genes
Bound by RBPJ
Not Bound by RBPJ
RBPJ ChIP on OLIG2 promoter
C
IgG
RBPJ
1% Input
1.5
1.0
0.5
0.0
**
**
3691
4121
D
RBPJ ChIP on FOXM1/OLIG2 promoter
DMSO
DAPT
% Input
1.5
1.0
0.5
0.0
FOXM1
OLIG2

Figure S7

A

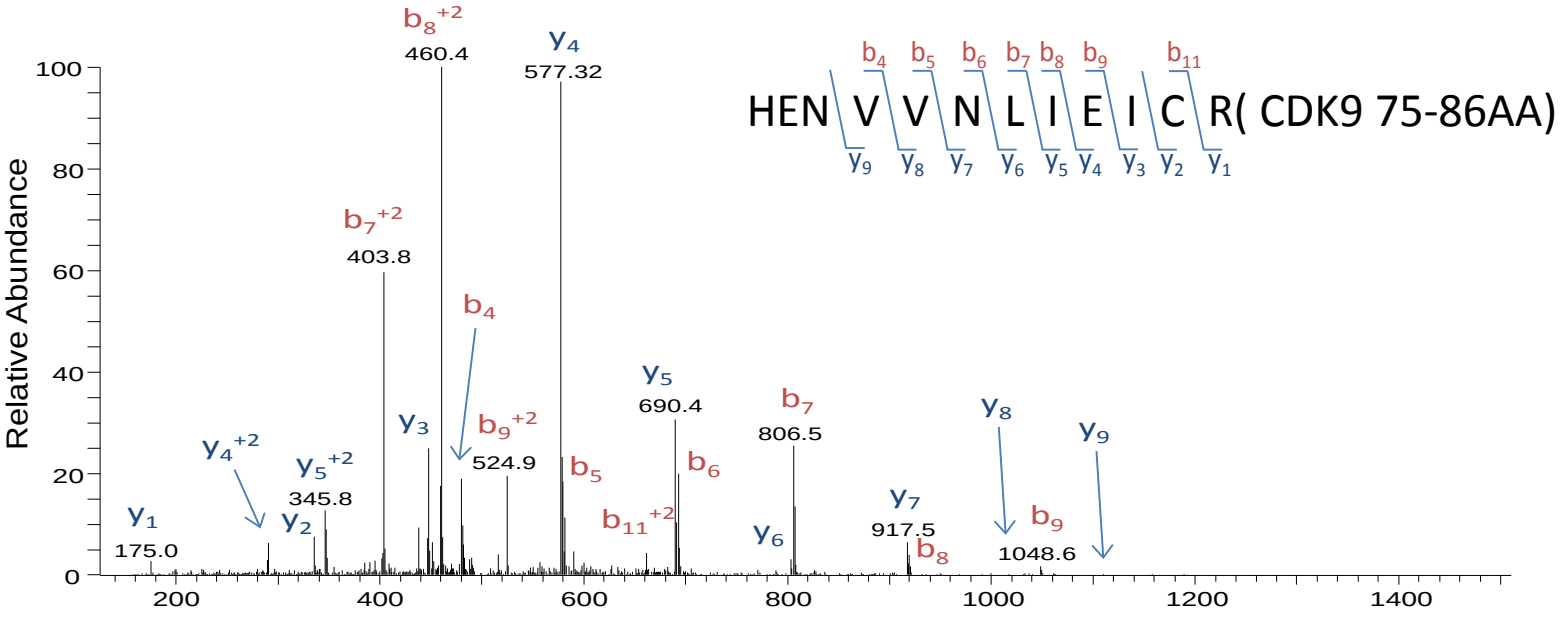
HEN V V N L I E I C R(CDK9 75-86AA)
Relative Abundance
b8+2 460.4
y4 577.32
b7+2 403.8
b4
y3
b9+2 524.9
y4+2
y5+2 345.8
y1 175.0
y2
b5
y5 690.4
b6
b11+2
b7 806.5
y6
y7 917.5
b8
y8
b9 1048.6
y9

B

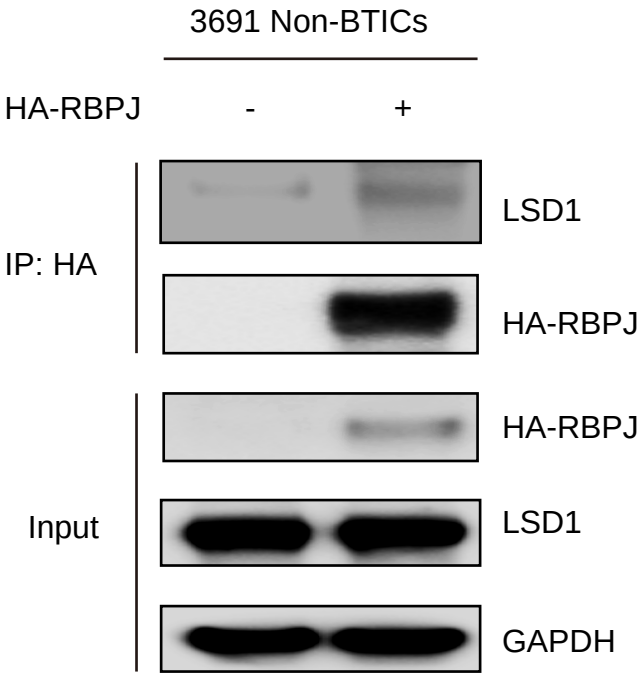
3691 Non-BTICs
HA-RBPJ - +
IP: HA
LSD1
HA-RBPJ
Input
HA-RBPJ
LSD1
GAPDH

Figure S8

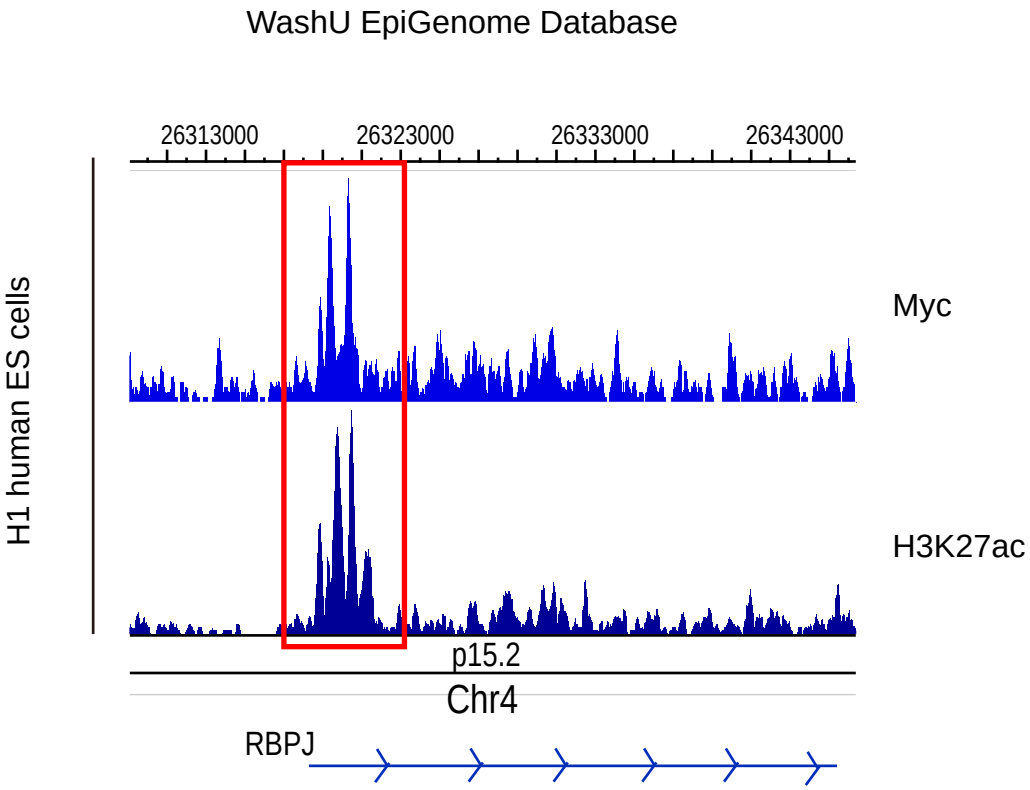
WashU EpiGenome Database
26313000
26323000
26333000
26343000
H1 human ES cells
Myc
H3K27ac
p15.2
Chr4
RBPJ

Figure S9

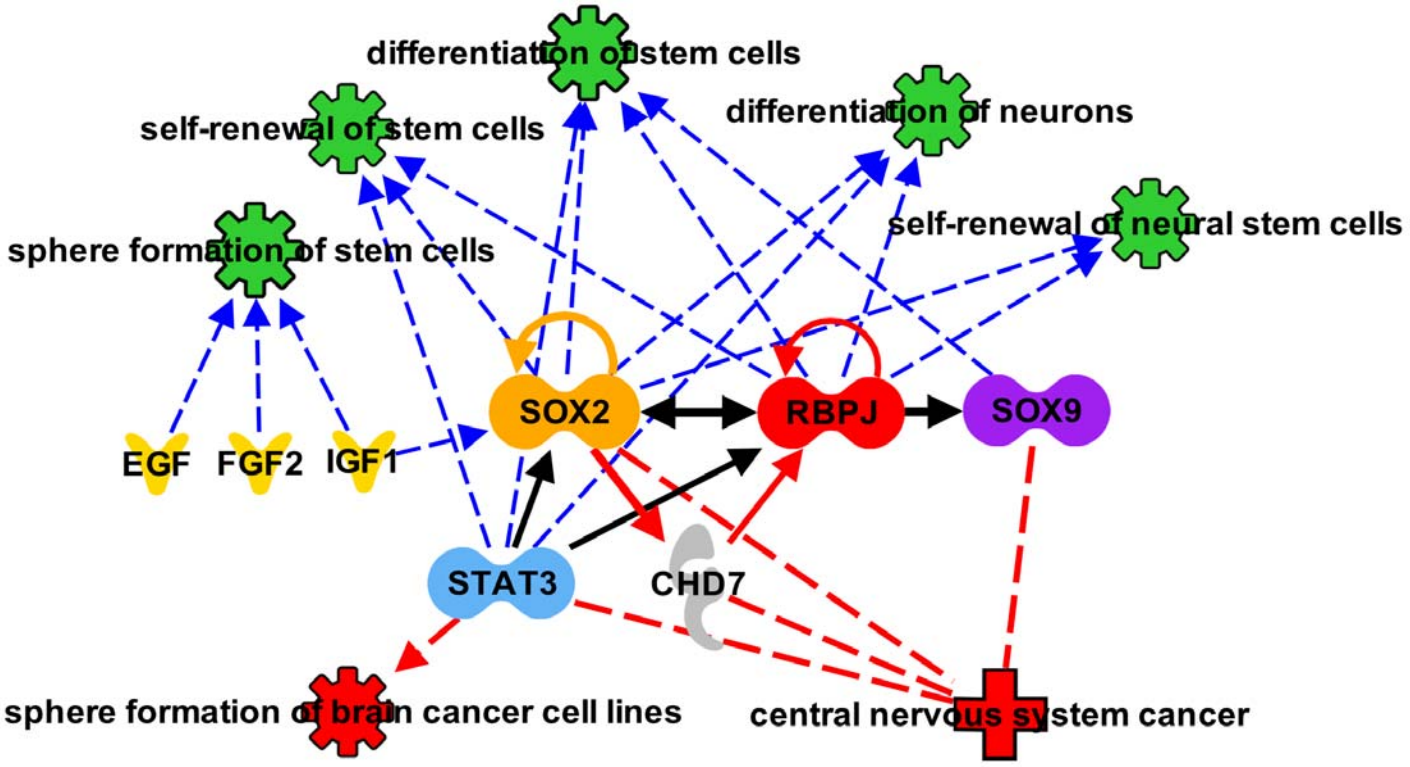
differentiation of stem cells
self-renewal of stem cells
differentiation of neurons
self-renewal of neural stem cells
sphere formation of stem cells
SOX2
RBPJ
SOX9
EGF
FGF2
IGF1
STAT3
CHD7
sphere formation of brain cancer cell lines
central nervous system cancer

Figure S10

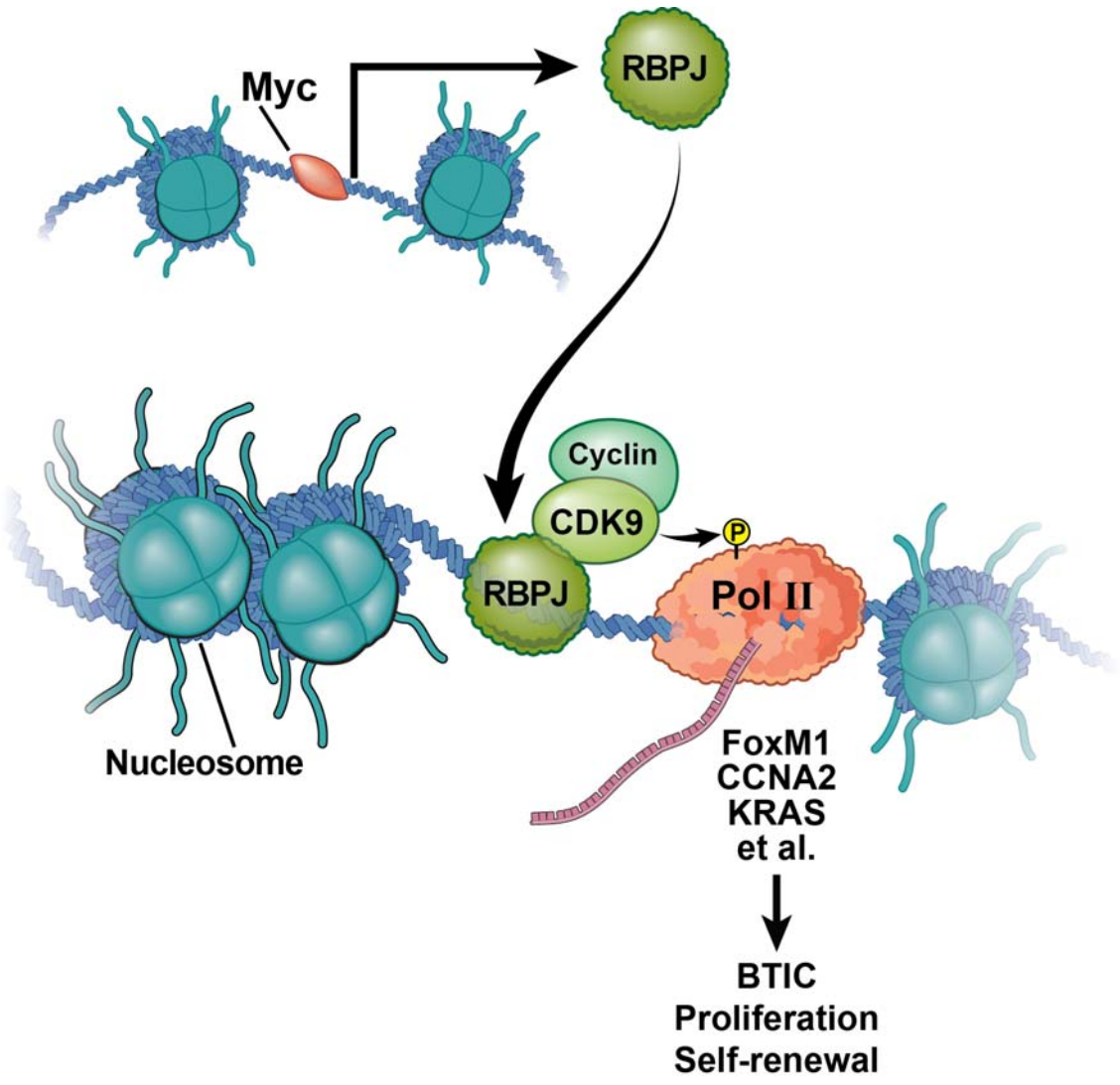
Myc
RBPJ
Cyclin
CDK9
P
RBPJ
Pol II
Nucleosome
FoxM1
CCNA2
KRAS
et al.
BTIC
Proliferation
Self-renewal

Full unedited gel for Figure 1C

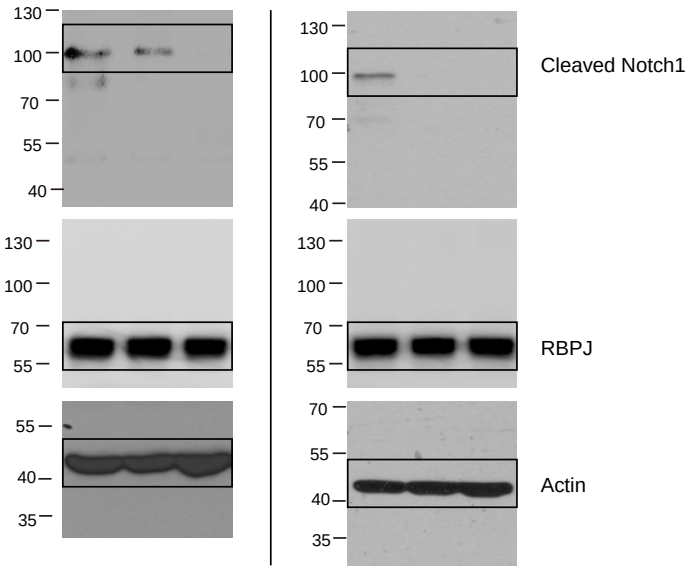

Full unedited gel Figure 2A

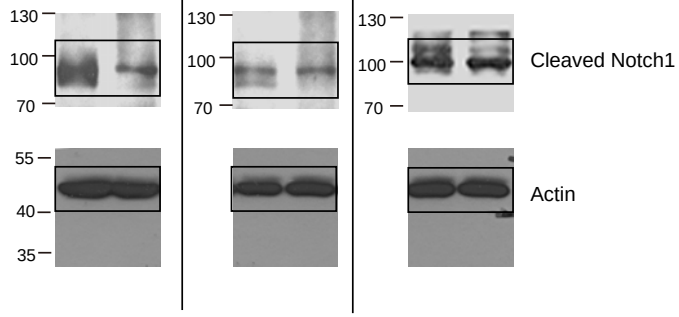

Full unedited gel Figure 2C

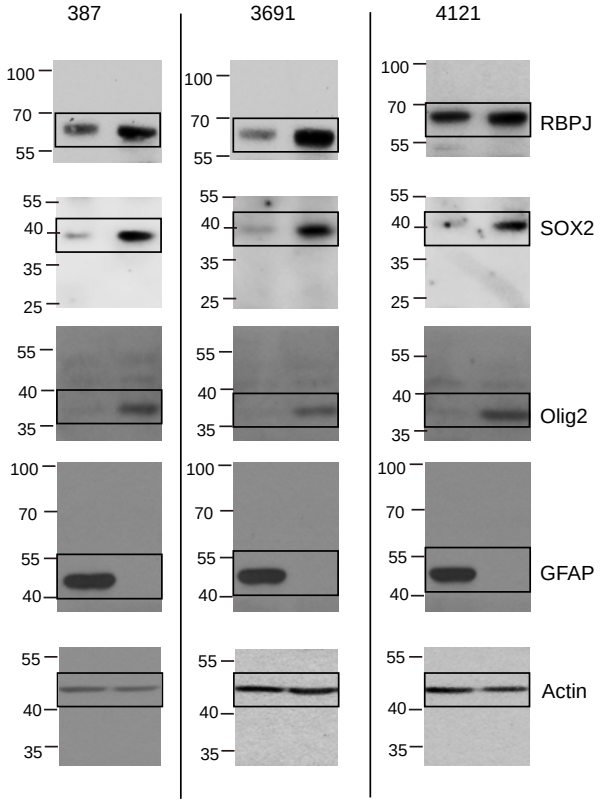

Full unedited gel Figure 2D

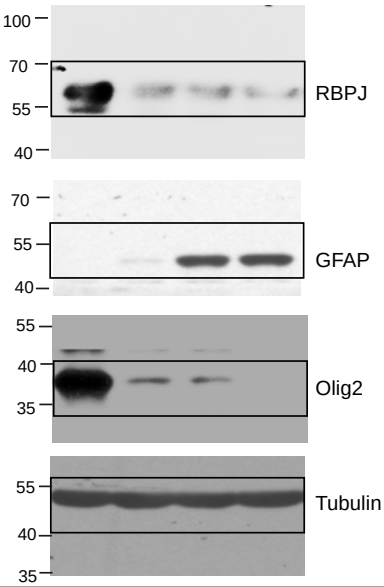

Full unedited gel Figure 3A, B

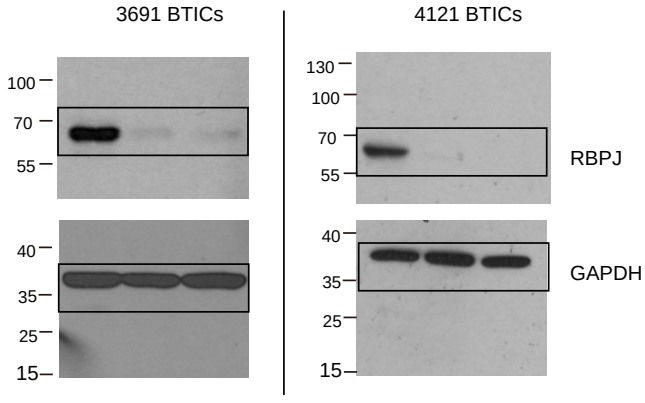

Full unedited gel Figure 6C

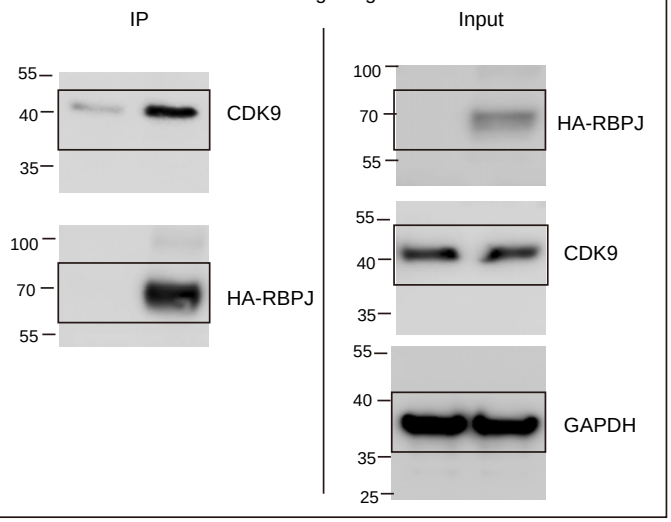

Full unedited gel Figure 7A

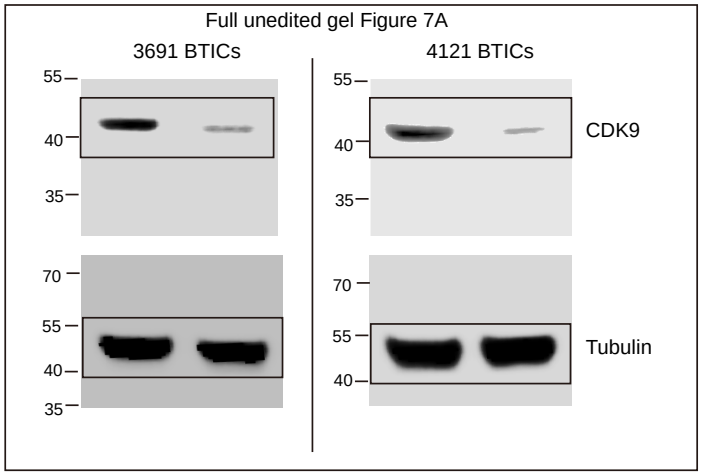

Full unedited gel Figure 8C

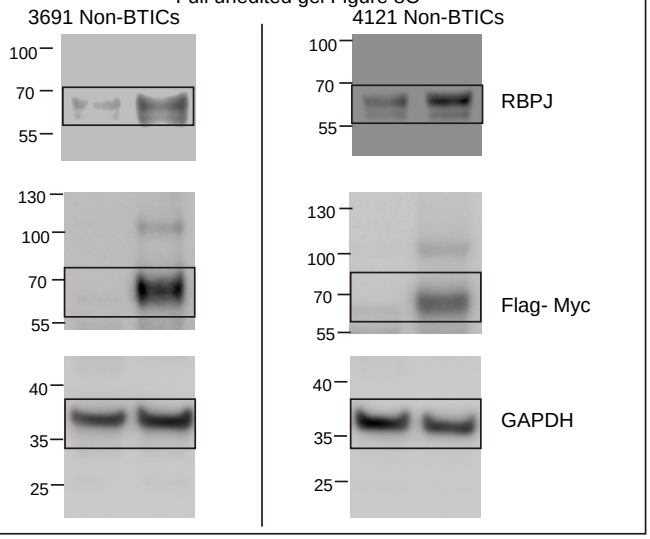

Full unedited gel Figure 8B

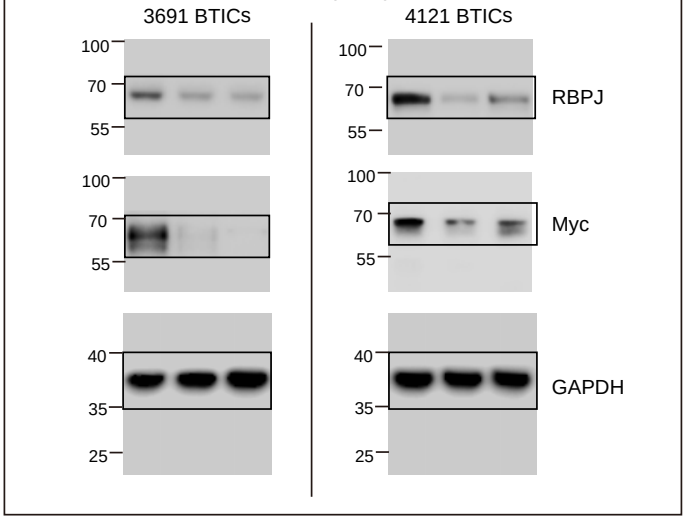

Full unedited gel Figure 8D

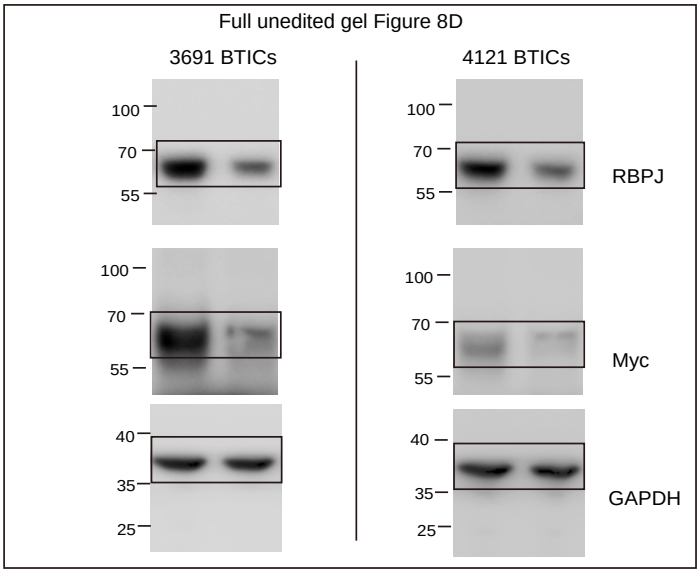

Full unedited gel Figure S2A

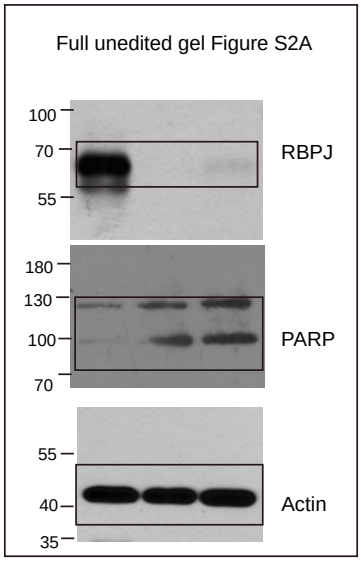
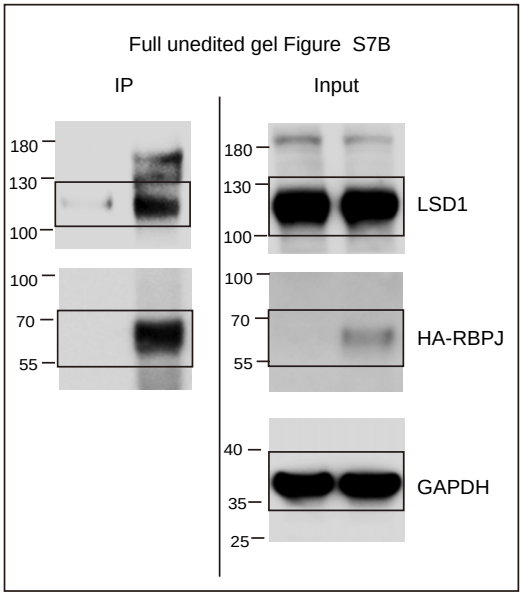
Full unedited gel Figure S7B